

Fault Tolerant Control of a Small Helicopter with Tail Rotor Failures in Forward Flight

Sulakshan Rajendran and Da-wei Gu

*Control Systems Research Group, Department of Engineering, University of Leicester
UK (e-mail: sulakshanrajendra@yahoo.com)
Department of Power Electronics and Automation, China Three Gorges University,
Hubei, People's Republic of China. (e-mail: dag@le.ac.uk)*

Abstract: Tail rotor failure is one of the major failures occurring frequently and causing accidents. In this paper we investigate Tail Rotor Control Failure (TRCF) based on helicopter dynamic models. There is no notable work reported in the literature on control of a small helicopter with TRCF. In contrast to hover mode, forward flight improves yaw damping naturally. The yaw damping is investigated at hover mode and in forward flight. Multi-loop PID controller, Fuzzy PID controller and full state feedback controller based on LQR are designed as per ADS-33PRF requirements to control the helicopter when the tail rotor control failure occurs in forward flight. Robustness in terms of stabilizing ability of developed controllers is also analyzed. All developed control schemes are tested in Matlab/Simulink environment including linear as well as non-linear simulations.

1. INTRODUCTION

Exploration of fault-tolerant control schemes of air vehicles has been greatly motivated by the growing concern as to the safety of Unmanned Air Vehicles (UAV) specially vertically Taking Off and Landing (VTOL) vehicles. Since the small-scale UAVs are frequently used in daily life, commercial and military activities and they are often operated in adverse environment, there are great concerns as how they would interact with manned air vehicles and the people on ground under failure situations. It is important to ensure the safety of people on ground and the VTOL vehicle from crashing on ground. Such considerations require the vehicles should be able to descend and land in a controlled mode when failure occurs.

Most critical failures that could occur to a VTOL vehicle are actuator lockout, tail rotor failure and motor failure. Generally in manned VTOL vehicles, sufficient fail-safes that the back-ups in most critical failures are designed. The payload capacity of a manned VTOL allows the mitigation technologies and redundant systems to be installed. These fail-safes includes mechanical and hydraulic devices to assist the pilot in reducing the required control effort to land the vehicles safely. The ongoing research on VTOL vehicles includes control of full-size (Amidi, 1996), giant scale (Johnson, et al., 2002), and miniature vehicles (Storvik, 2003). Full-size and giant vehicles are usually manned vehicles and possible solutions require special clearance approved by civil and military aviation authorities of respective airspace, for an example, Federal Aviation Administration (FAA) in USA and Civil Aviation Authority (CAA) in UK. However UAV VTOL vehicles do not have the luxury of back-ups due to the restricted payload though they are capable of autorotation. Though VTOL

makes up a dispensable part of daily life, the research on UAV VTOL vehicles safety issues is still relatively new regarding surviving-critical failures. So it is thus understandable it has become a much of targeted area of research.

This paper focuses on Tail Rotor Control Failure (TRCF) and it is observed there is almost no work addressing TRCF in the literature. However control schemes to control rotorcraft during autorotation more specifically during vertical autorotation are discussed in a few papers. There is one notable controller designed in the tail-rotor failed mode based on fuzzy logic (Garcia, et al., 2007). It discusses on navigating the rotorcraft with completely lost tail rotor allowing it to spin through out the navigation. Though the software recovery on UAVs is still a very much new area, there are some attempts made at Georgia Tech. It is shown that Rmax vehicle still could be controlled under main rotor collective actuator lock out (Kannan, et al., 1999) and swash plate actuator lock out (Johnson, et al., 2005). Both attempted to control the rotorcraft with remaining actuators and showed that software enabled control is possible. There are more work on emergency landing by autorotation, (Dalamagkidis, et al., 2009) developed a controller based on Model Predictive Control scheme (MPC) to perform vertical autorotation. In this paper controllers based on PID, Fuzzy PID and LQR are designed to control the helicopter when TRCF occurs.

The layout of the present paper is as following. Section 2 presents the detailed conceptual nature of tail rotor failures. Section 3 describes the mathematical model used in controller design procedure. The nature of yaw movement in forward flight is investigated in section 4. The multi-loop PID controller is presented in section 5. Section 6 presents the

controller designed based on LQR. Simulations with both linearised and non linear models are presented in 5 and 6 for respective schemes. And finally in section 7 conclusions are presented.

2. ON TAIL ROTOR FAILURES

Tail- rotor is an integrated feature of conventional helicopters with single main rotor. The primary function of a tail rotor is to counteract the torque produced by the main rotor. If due to any reason, tail rotor fails to produce required anti-torque then the helicopter would experience yaw movement depending on main rotor's rotating direction. Tail rotor failures are primarily classified into two types. The first one is, Tail Rotor Drive Failure (TRDF) in which tail rotor stops spinning and no anti-torque is produced, the general recovery action is autorotation. The engine is shut down and the rotorcraft is allowed to descend. The second one is Tail Rotor Control Failure (TRCF). In the TRCF mode the tail rotor continues to spin but the tail rotor thrust produced cannot be altered by specifying desired tail rotor collective pitch. This also described frozen control state. The necessary recovery action varies for each failure upon flight mode and operating power. This situation can be shown as in a flow chart in Fig.1.

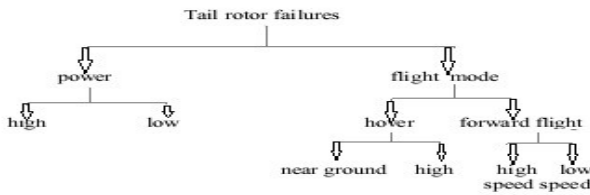


Fig.1. Flowchart: Classification of Tail rotor failures

In this paper TRCF is the case to be addressed and TRDF is not discussed further. In TRCF mode the pedal is unmovable and the pitch angle of tail rotor blade is stuck. It could occur due to broken control rod or object interference with pedals. It is classified into further three cases. They are low stuck pitch/right stuck pedal, neutral stuck pitch/neutral pedal and high stuck pitch/left stuck pedal. A realistic immediate response of a manned rotorcraft is sudden yaw movement to right or left depending on main rotor rotating direction and the stuck type. General recovery action implemented by a human pilot is rolling off the throttle to decrease the main rotor torque if stuck pedal is such that the anti-torque is less than main rotor torque. If the stuck pedal results in anti torque greater than main rotor torque then collective is applied in a way so that the main rotor torque increases. The recovery actions taken by the pilot varies with flight mode. During stuck neutral, the throttle is rolled to lower the power. And the rotorcraft is allowed to descend. Reduced power produces yaw due to anti-torque greater than the main rotor torque. This is rectified by applying collective to increase main rotor torque. The recovery actions to handle the low pitch/right stuck are very much alike as to neutral.

3. MATHEMATICAL MODEL

Linear Mathematical model developed by (Metter, et al.2000) is used directly without derivation. Linear dynamic equations are given below.

$$\dot{u} = (-w_0q + v_0r) - g\theta + X_uu + X_wa \tag{1}$$

$$\dot{v} = (-u_0r + w_0p) + g\phi + Y_vv + Y_b b \tag{2}$$

$$\dot{p} = L_uu + L_vv + L_b b \tag{3}$$

$$\dot{q} = M_uu + M_vv + M_a a \tag{4}$$

$$\dot{w} = (-v_0p + u_0q) + Z_w w + Z_{col} \delta_{col} \tag{5}$$

$$\dot{r} = N_r r + N_{ped} \delta_{ped} \tag{6}$$

$$\dot{\theta} = q \tag{7}$$

$$\dot{\phi} = p \tag{8}$$

u,v and w are translational velocities and θ, ϕ are attitude angles. Then p, q and r are angular rates. The rotor derivatives are X_u, Y_b and the rotor moments through the flapping spring derivatives are L_b, M_a . General aerodynamic effects are expressed by speed derivatives such X_u, X_w, M_u, M_v . And Z_{col}, N_{ped} are control derivatives. The above equations are formulated in standard state space Equation (9).

$$\dot{X} = Ax + Bu \tag{9}$$

$$Y = Cx + Du$$

where x,u and y are

$$x = \{u, v, p, q, \phi, \theta, w, r\}^T$$

$$u = \{\delta_{lat}, \delta_{lon}, \delta_{ped}, \delta_{col}\}^T$$

$$y = \{u, v, \phi, \theta, w, r\}^T$$

The 13th order model is reduced to 8th order to design controller based on classical multi-loop PID controller. Firstly the yaw rate feedback is eliminated. Then the flapping of rotor and the stabilizer bar are assumed to be in steady state and then substituted in angular rate equations. The state space representation of reduced order model is given in equation (10).

The developed controllers are tested with a nonlinear model using the HeliSim software (AAU Helisim) developed by Aalborg university. Non linear simulation diagram is given in Fig.2.

$$\begin{bmatrix} \dot{u} \\ \dot{v} \\ \dot{p} \\ \dot{q} \\ \dot{\phi} \\ \dot{\theta} \\ \dot{w} \\ \dot{r} \end{bmatrix} = \begin{bmatrix} X_u & 0 & 0 & 0 & 0 & -g & 0 & 0 \\ 0 & Y_v & 0 & 0 & 0 & g & 0 & 0 \\ L_u & L_v & -L_b(\tau_r - B_d \tau_s) & 0 & 0 & 0 & L_w & 0 \\ M_u & M_v & 0 & -M_a(\tau_r + A_c \tau_s) & 0 & 0 & M_w & 0 \\ 0 & 0 & 1 & 0 & 0 & 0 & 0 & 0 \\ 0 & 0 & 0 & 1 & 0 & 0 & 0 & 0 \\ 0 & 0 & 0 & 0 & 0 & 0 & Z_w & Z_r \\ 0 & N_v & N_p & 0 & 0 & 0 & N_w & N_r \end{bmatrix} \begin{bmatrix} u \\ v \\ p \\ q \\ \phi \\ \theta \\ w \\ r \end{bmatrix} + \begin{bmatrix} 0 & 0 & 0 & 0 \\ 0 & 0 & Y_{ped} & 0 \\ L_b(B_{lat} + B_d P_{lat}) & L_b P_{lon} & 0 & 0 \\ M_a A_{lat} & M_a(A_{lon} + A_c C_{lon}) & 0 & M_{col} \\ 0 & 0 & 0 & 0 \\ 0 & 0 & 0 & 0 \\ 0 & 0 & 0 & 0 \\ 0 & 0 & N_{ped} & N_{col} \end{bmatrix} \begin{bmatrix} \delta_{lat} \\ \delta_{lon} \\ \delta_{ped} \\ \delta_{col} \end{bmatrix} \tag{10}$$

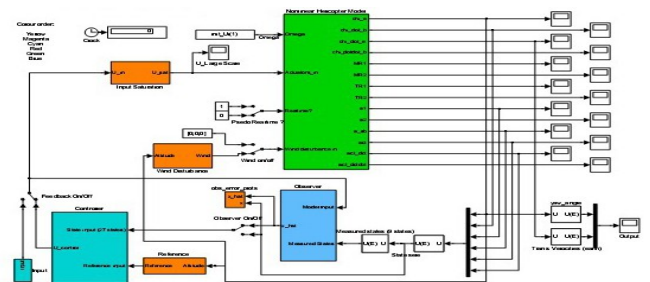


Fig.2. Nonlinear simulation model

3. YAW NATURE IN FORWARD FLIGHT

In contrast to hover mode the helicopter shows good directional stability in forward flight. This is because the forward speed generates streaming line effect which improves yaw damping naturally. To investigate this, the helicopter is initialised at hover and forward flight and then pedal doublet input is given as yaw disturbance. It is repeated at different forward speeds. The yaw responses are given in Fig.3.

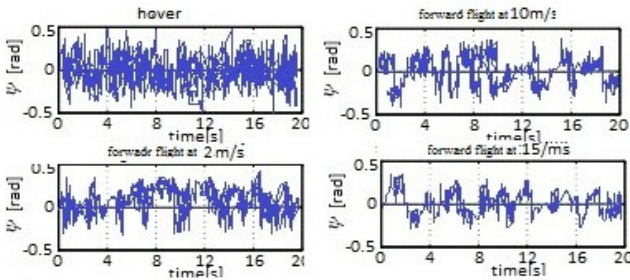


Fig.3. Yaw responses at hover and forward flight at 2m/s, 10m/s and 15m/s.

It is observed that at hover, yaw oscillations are severe and in forward flight it reduces with increasing speed.

5. PID APPROACHES

5.1 Classical PID controller

MIMO system is transformed into four SISO systems to design PID controllers for each channel. The state space model described in equation (8) is decoupled into four channels. They are longitudinal, lateral, heave and yaw channels. Firstly the longitudinal channel is designed. The multi-loop structure of longitudinal channel is shown in Fig.4.

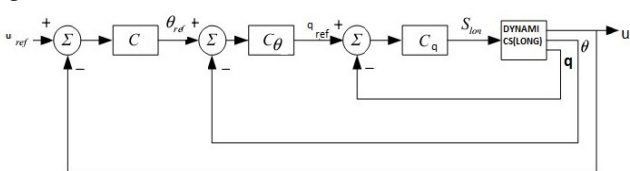


Fig.4. Longitudinal channel

Ziegler-Nichols “Ultimate Sensitivity method”(Franklin, *et al.*, 2002) will be used to find P,I and D gains in each case. The procedure is to set I and D to Zero, and then P is increased until the output of the closed loop system is oscillating with a constant amplitude. This happens when pole is placed on imaginary axis of complex plane. This gain is called “ultimate gain K_u ” and the period of oscillations is called P_u . Having these values PID gains are tuned according to Table.1.

Table.1. Ziegler-Nichols scheme for tuning PID controller

Control type	P	I	D
P	$0.5K_u$	$0.45K_u$	$0.6K_u$
I	-	$0.54K_u/P_u$	$1.2K_u/P_u$
D	-	-	$0.075K_u/P_u$

The Lateral and yaw channels of fully operational helicopter are designed similarly as longitudinal and heave channels.

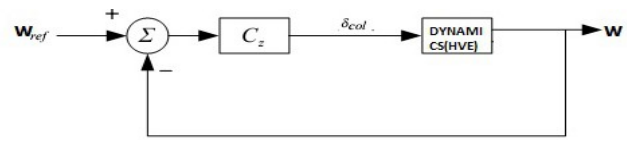


Fig.5. Heave channel

In TRCF mode the yaw channel is augmented in lateral channel. The procedure is explained below. The fault-free decoupled yaw dynamics is given in equation (11).

$$\dot{r} = N_r r + N_{ped} \delta_{ped} \quad (11)$$

In TRCF mode pedal input is zero. So the Fault is modelled by removing the pedal input in equation(9). And the lateral velocity influence on yaw dynamics is augmented. So the new augmented yaw dynamics is given in equation (12).

$$\dot{r} = N_r r + N_V V \quad (12)$$

The three loop structure of lateral control is now extended to further two in outer loop. The yaw rate PID controller is responsible for generating v_{ref} to the next lateral velocity loop. Heading controller is designed in the outer most loop to generate yaw rate reference. The augmented lateral/yaw channel is given in Fig.7.

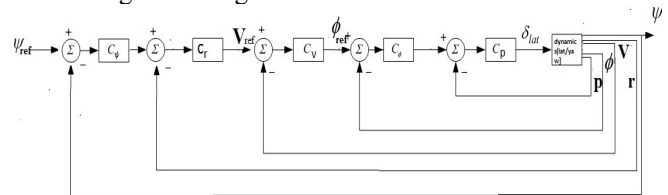


Fig.7. Lateral/Yaw augmented channel

The obtained PID gains are given in table.2.

Table.2. Controller gains

Control variable	P	I	D
u	0.05	0.38	0
theta	-1	0	0
q	1.23	0.45	0.96
v	1.03	0.69	0
phi	-1	0	0
p	1.18	0.36	0.78
r	1.37	0.46	0.13
psi	2	0	0
w	0.46	0.28	0

The linear simulation results are presented in Fig.8.

5.2 Fuzzy PID controller

The success of the PID controller depends on right choice of gains. An appropriate method of tuning PID gains assures good performance of the controller. The fuzzy PID controller uses the classical PID controller as the foundation which uses the fuzzy reasoning and variable universe of discourse to regulate the PID gains. The beneficial properties such as robustness and adaptability of a fuzzy system can be incorporated into control method for better tuning of PID gains. The general block diagram fuzzy PID controller is given in Fig.9. In TRCF condition, side velocity of the helicopter is the only source of controlling yaw apart from

collective/rotor speed variation management. It is discussed in classical PID design, the yaw controller that is augmented in lateral channel is responsible for generating v reference and it is the key part of the whole channel. So it is replaced with fuzzy PID to see the performance improvements. In view of the different error e and error rate, different PID control parameters of K_i , K_d , K_p are demanded, and we set rules as follows.

1) When $|e|$ is big, for the system to have good tracking performance, we should take large K_p and small K_d ;

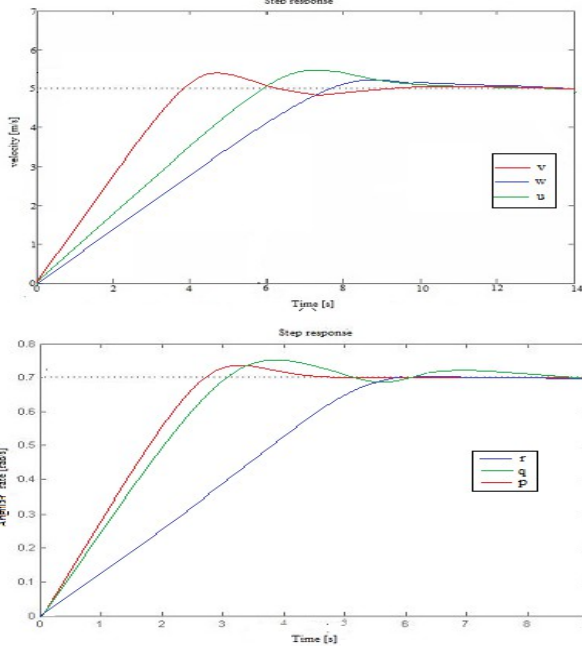


Fig.8. Linear simulation results of classical PID controller

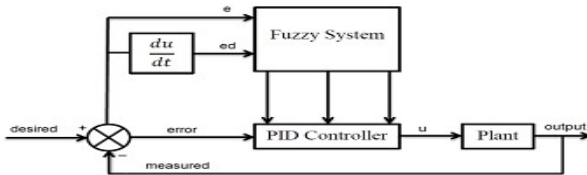


Fig.9. Fuzzy PID controller

meanwhile, in order to avoid large overshoot in system response, we should set a limit to the integral effect, usually we take $K_i = 0$.

2) When $|e|$ and $|ec|$ are median size, for the system to have a small overshoot, we should take small K_p . In this case, K_d is bigger impact on the system, we should take a small value, K_i should be proper.

3) When $|e|$ is small, for the system to have a good stability, we should take big K_i and K_d ; meanwhile, in order to avoid appearing oscillation within the set value, and considering anti-interference performance of the system, when $|ec|$ is large, K_d should be taken a smaller value, and vice versa (Shiyong, *et al.*, 1998).

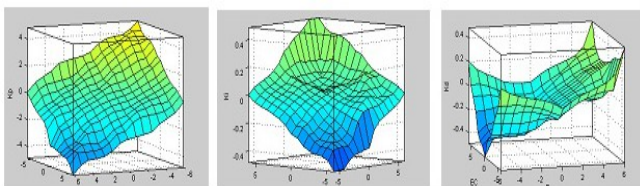


Fig.10. Three-dimensional diagrams of rules of K_p , K_i and K_d .

The membership function of all inputs and outputs are selected as identical and they are combination of triangular and Gaussian. It is shown in Fig.11. The width of fuzzy sets are not the same and they are determined by trial and error. The range of K_p is chosen as $[0.5 \ 1.5]$, K_i is $[0.1 \ 0.5]$ and K_d is $[0.05 \ 0.4]$. The ranges of inputs error and error rate are $[-1 \ 1]$ and $[-10 \ 10]$.

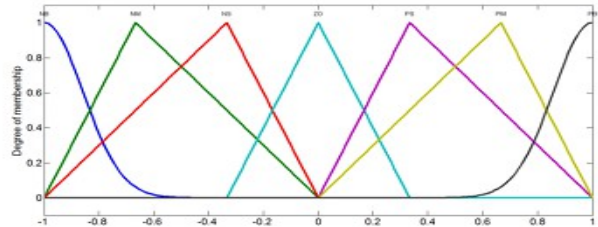


Fig.11. Membership functions

The defuzzification is done by centroid defuzzifier to have high membership degree that approximately corresponds to the middle of the graph. The rules of K_p is given in Table.3 and the rules of K_i and K_d is in Table.4 and Table.5 respectively.

Table.3. Rules of K_p

		Error						
		NB	NM	NS	ZO	PS	PM	PB
Errorrate	NB	PB	PB	PM	PM	PS	ZO	ZO
	NM	PB	PB	PM	PS	PS	ZO	NS
	NS	PM	PM	PM	PS	ZO	NS	NS
	ZO	PM	PM	PS	ZO	NS	NM	NM
	PS	PS	PS	ZO	NS	NS	NM	NM
	PM	PS	ZO	NS	NM	NM	NM	NB
	PB	ZO	ZO	NM	NM	NM	NB	NB

Table.4. Rules of K_i

		Error						
		NB	NM	NS	ZO	PS	PM	PB
Errorrate	NB	NB	NB	NM	NM	NS	ZO	ZO
	NM	NB	NB	NM	NS	NS	ZO	ZO
	NS	NM	NM	NS	NS	ZO	PS	PS
	ZO	NM	NM	NS	ZO	PS	PM	PM
	PS	NM	NS	ZO	PS	PS	PM	PB
	PM	ZO	ZO	PS	PS	PM	PB	PB
	PB	ZO	ZO	PS	PM	PM	PB	PB

Table.5. Rules of K_d

		Error						
		NB	NM	NS	ZO	PS	PM	PB
Errorrate	NB	PS	NS	NB	NB	NB	NM	PS
	NM	PS	NS	NB	NM	NM	NS	ZO
	NS	ZO	NS	NM	NM	NS	NS	ZO
	ZO	ZO	NS	NS	NS	NS	NS	ZO
	PS	ZO	ZO	ZO	ZO	ZO	ZO	ZO
	PM	PB	NS	PS	PS	PS	PS	PB
	PB	PB	PM	PM	PM	PS	PS	PB

The linear results produced by fuzzy PID controllers are shown in Fig.12. It can be seen in Figure.13 that the PID controller produces yaw response that is just outside the level 1 requirements. The fuzzy PID controller manages to keep the yaw response within the level 1 region.

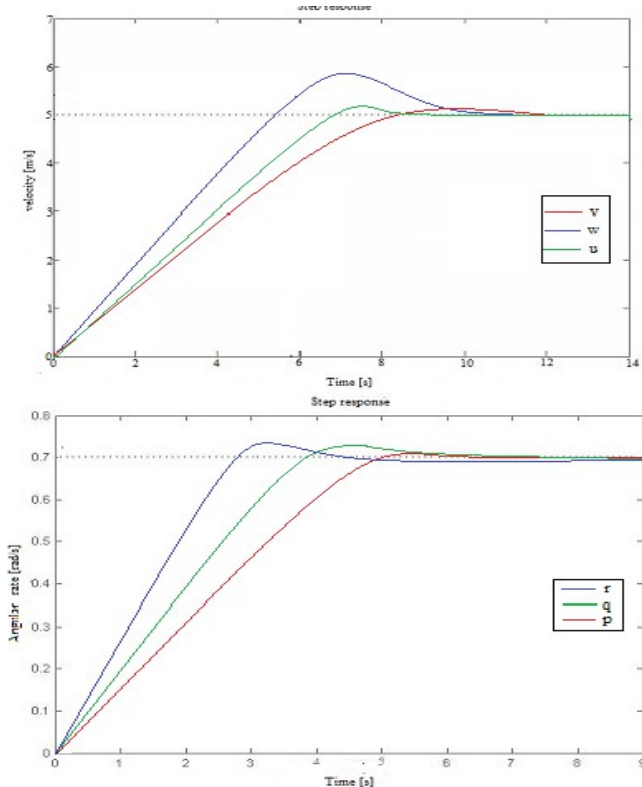


Fig.12. Linear results of Fuzzy PID controller

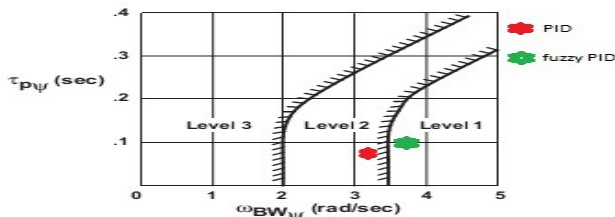


Fig.13. Requirement for small-amplitude yaw response for Target Acquisition and Tracking –forward flight, ADS-33E-PRF.

Non linear simulation results of classical PID controller are given in figure.14.

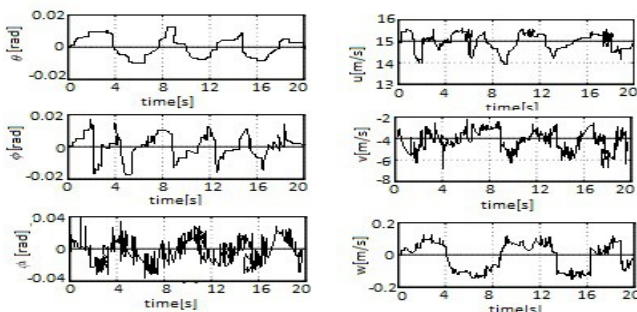


Fig.14. Non linear simulation results of PID controller

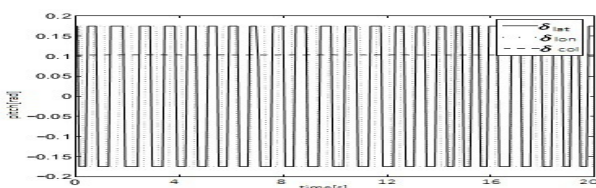


Fig.15 Control efforts of PID controller

PID controller stabilizes the helicopter when applied to a non linear model. But it exhibits large vibrations specifically in yaw angle and lateral velocity. In Fig.15 very high control efforts of lateral and longitudinal cyclic controls are observed.

6. LQR CONTROLLER DESIGN

The reduced 8th order model given in equation (8) is used. And to model the TRCF condition, the pedal control input column is eliminated. So resulting input “u” and state “x” vectors are

$$x = [u \ w \ q \ \theta \ v \ p \ r \ \varphi]^T$$

$$u = [\delta_{col} \ \delta_{lng} \ \delta_{lat}]^T$$

Controllability of the system is verified.

In LQR approach the state space equation (13) is solved using the cost function.

$$J(x,t) = \int_0^{\infty} (x^T Q x + u^T R u) d\tau$$

Where Q and R are positive definite matrix. Firstly initial Q and R matrix has to be chosen to perform trials to determine the optimal values to find the K matrix that stabilizes the linear system.

Q is diagonal with $Q_{ij} = 1/\max\{x_i(k)^2\}$

R is diagonal with $R_{ij} = 1/\max\{u_i(k)^2\}$

After number of trials the final Q and R matrix are

$Q = \text{diag}([1.7255 \ 0.1545 \ 0.233 \ 0.9221 \ 0.75 \ 0.78 \ 1.8 \ 0.9])$;

$R = \text{diag}([1 \ 1 \ 1])$;

$K_{lqr} = (A \ B \ Q \ R)$;

Linear simulation results are presented below.

$$K = \begin{bmatrix} -2.227 & 3.445 & 1.775 & 0.3566 & 1.366 & 4.677 & 2.0345 & 1.2557 \\ -0.255 & 2.789 & 3.409 & 1.0223 & 5.222 & 12.45 & 9.3455 & 21.991 \\ 2.335 & 8.234 & 7.234 & 0.9877 & 7.123 & 8.125 & 12.456 & 18.752 \end{bmatrix}$$

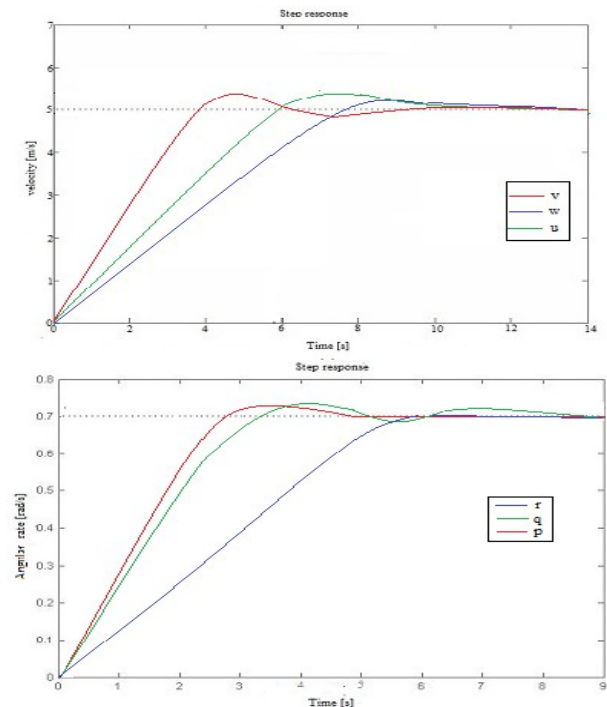


Fig.13. Linear simulation results of LQR controller

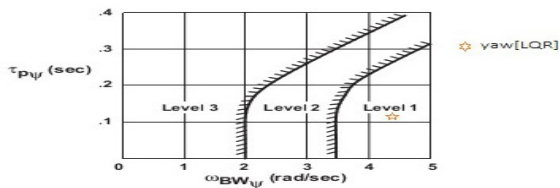


Fig. 14. Requirement for small-amplitude yaw response for Target Acquisition and Tracking –forward flight, ADS-33E-PRF

The LQR controller keeps the yaw response well within the level 1 region as seen in Fig. 14.

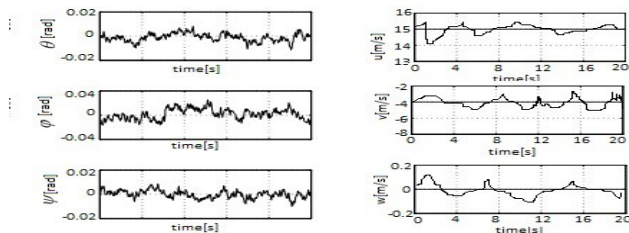


Fig. 15. Non linear simulation results of LQR controller

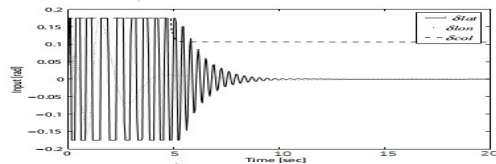


Fig. 16. Control efforts of LQR controller

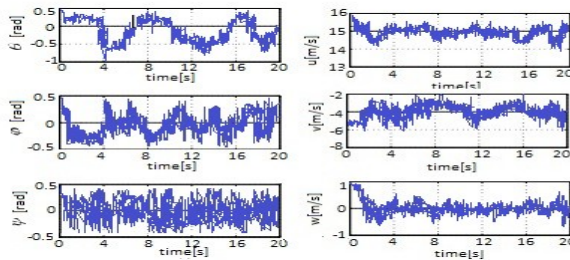


Fig. 17. Simulation results when initialized with offsets (LQR)

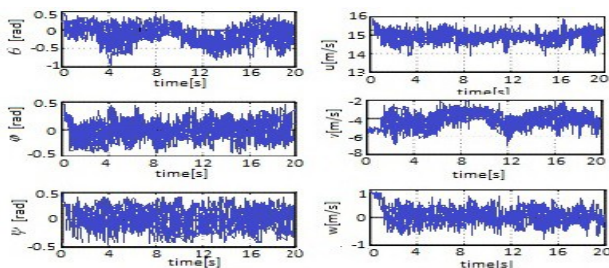


Fig. 18. Simulation results when initialized with offsets (PID)

The LQR controller produces better results overall than the PID controller. The variations and vibrations in angles and velocities are reduced. Specifically the lateral velocity and yaw angle show less variation and vibration. The control efforts are much lesser than PID controller. The LQR controller showed better performance than the PID controller when tested at the operating point. The Robustness of the controllers in stabilizing the helicopter is investigated by performing the nonlinear simulation giving offsets of 0.5 rad for angles and 1 m/s for velocities. The results are given in Figure.17 and 18. It can be seen that only longitudinal and

vertical velocities are stabilized with intense vibrations. The LQR controller showed less vibrations compared to PID. But both LQR and PID controllers fail to stabilize the attitude angles and lateral velocity.

7. CONCLUSIONS

Developed controllers successfully stabilized the helicopter with TRCF in forward flight. All the controllers presented in this paper are able to keep up with the ADS-33-PRF requirements in forward flight. The marginal performance of classical PID controller is enhanced by the self-tuning fuzzy system. The LQR controller shows better results among the three controllers in both linear and non linear simulations. But both LQR and PID controllers do not exhibit sufficient robustness when they are applied in the case of giving offsets to the operating point. The LQR controller shows slightly better robustness compared to PID controller. So in future work more robust control techniques will be used to incorporate robustness explicitly in design.

REFERENCES

- AAU HeliSim, Aalborg University, 2009, <http://uavlab.org>.
- Amidi, O. (1996). An Autonomous Vision-Guided Helicopter, M.A. thesis, Carnegie Mellon University
- Barry, J., Baskett, (2000). Handling Qualities Requirements for Military Rotorcraft, US Army AVSCOM Aeronautical Design Standards, ADS-33E-PRF.
- Dalamagkidis, K., Valavanis, K., P., and Pigel, L., A., (2009). Autonomous Autorotation of an Rotorcraft using non linear Model Predictive Control, *Journal of Intelligent and Robotic Systems*, Vol.57, pp. 351–369.
- Garcia, R., D., Valayanis, K., P and Kandel, K. (2007.) Autonomous helicopter navigation during tail rotor failure utilizing Fuzzy logic, *Mediterranean Conference on Control and Automation*.
- Johnson, E., Mishra, S. (2002). Flight Simulation for the development of an experiment UAV, *AIAA Modelling and Simulation Technologies Conference and Exhibit*.
- Johnson, E., Schrage, D., and Vachtsevanos, G., (2005). Rotary Wing Final Experiments for the Software Enabled Control Program. *Proceedings of the American Helicopter Society 61st Annual Forum*, Grapeview, TX, USA.
- Kannan, S., Restrepo, C., Yavrucuk, I., Willis, L., Scharge, D., and Prasad, J.V.R., (1999). Control algorithm and flight simulation integration using the open control platform for unmanned aerial vehicles, in *Proc. 18th Digital Avionics Systems Conference.*, St. louis, pp. 6.A.3-1--- 6.A.3-10.
- Metter, B., Tishler, M., B., and Kanade, T., (2000). System Identification Modelling of a Model-scale Helicopter, Technical Report CMU-RI-TR-00-03, Robotics Institute, CMU.
- Shiyong Li, (1998) *Fuzzy neural control and intelligent control theory*. Helilongjiang: Harbin Institute of Technology Press.
- Storvik, M. (2003). Guidance System for Automatic Approach to a Ship, M.A thesis, Norwegian University of Science and Technology.